Detailed crystal chemistry and iron topochemistry of asbestos occurring in its natural setting: A first step to understanding its chemical reactivity

ARTICLE *in* CHEMICAL GEOLOGY · OCTOBER 2010

Impact Factor: 3.52 · DOI: 10.1016/j.chemgeo.2010.07.018

3 AUTHORS, INCLUDING:

Giovanni B Andreozzi
Sapienza University of Rome
81 PUBLICATIONS **694** CITATIONS

SEE PROFILE

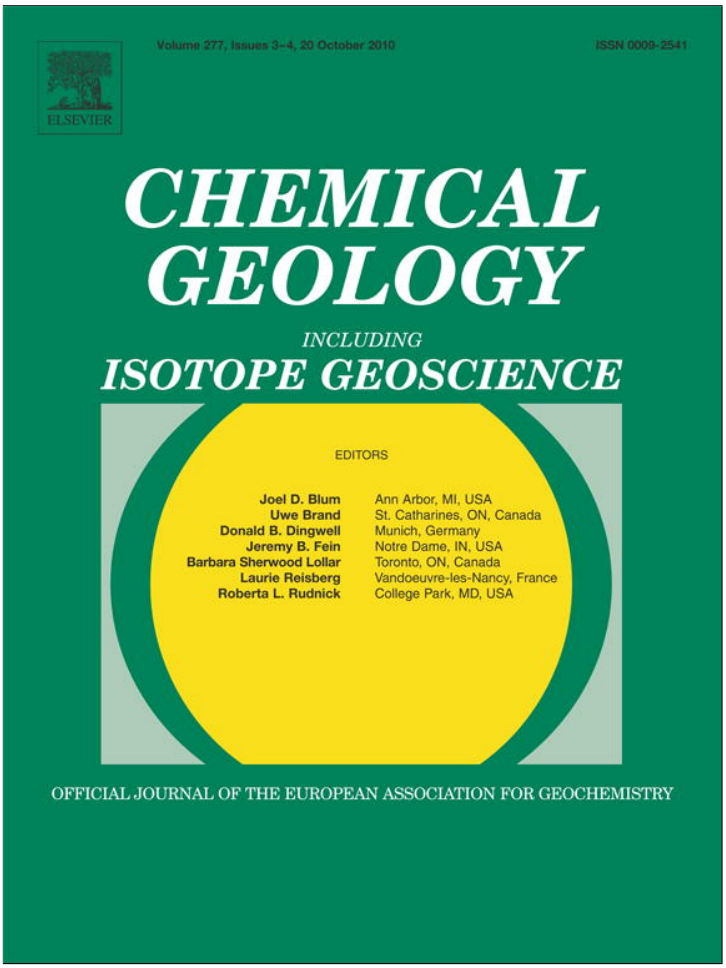

Chemical Geology 277 (2010) 197–206

Contents lists available at ScienceDirect

Chemical Geology

journal homepage: www.elsevier.com/locate/chemgeo

Detailed crystal chemistry and iron topochemistry of asbestos occurring in its natural setting: A first step to understanding its chemical reactivity

A. Pacella [a,*], G.B. Andreozzi [a], J. Fournier [b]

[a] Dipartimento di Scienze della Terra, Sapienza Università di Roma, Piazzale Aldo Moro 5, 00185 Roma, Italy
[b] UPMC Univ Paris 06, UMR 7197, Laboratoire de Réactivité de Surface, F-75005, Paris, France

ARTICLE INFO

Article history:
Received 19 May 2010
Received in revised form 26 July 2010
Accepted 27 July 2010

Editor: D.B. Dingwell

Keywords:
Tremolite
Asbestos
Crystal chemistry
Iron topochemistry
Reactive oxygen species
Hydroxyl radical

ABSTRACT

Five samples of tremolite asbestos from Italy and USA were fully characterized by ICP-MS, SEM, EMPA, FT-IR, MS, XRPD, to correlate crystal chemistry with chemical reactivity. Iron topochemistry was investigated in detail, due to the role of Fe in the aetiology of respiratory inflammatory diseases. The Italian tremolite samples have different Fe contents (San Mango>Ala di Stura>Rufeno>Castelluccio Superiore), and the USA sample from Maryland shows a value almost double that of the Italian samples. The bulk Fe^{3+}/Fe_{tot} ratio was quantified by Mössbauer spectroscopy, and the values obtained range from 6% Fe_{tot} (San Mango tremolite) to 24% Fe_{tot} (Mt. Rufeno tremolite). A possible site distribution of Fe was derived from combining chemical, spectroscopic (Mössbauer) and structural (Rietveld refinement) data. For all samples Fe^{2+} was disordered over M(1), M(2) and M(3) sites, whereas Fe^{3+} was allocated to M(2). Production of HO° radical in the presence of hydrogen peroxide from the Italian samples is a measure of chemical reactivity, with the lowest value observed for the Castelluccio Superiore sample, and the highest value for the San Mango sample. Notably, HO° radical production is directly related to the Fe occupancy of the M(1) and M(2) octahedra, which are more exposed on the external surface of the fibers than M(3) octahedra and therefore have higher probability of being involved in surface reactions.

1. Introduction

The present work deals with asbestos occurring in its natural setting. Of the six minerals with asbestiform habit regulated worldwide as asbestos (tremolite, actinolite, amosite, antophyllite, crocidolite and chrysotile) the phyllosilicate chrysotile and the fibrous amphiboles belonging to the tremolite–actinolite series are more widely distributed as minor constituents of metamorphosed mafic, ultramafic and carbonate rocks. The environmental relevance of asbestos is very high as both weathering and human activity can separate fibers and break them down to fibrils of submicroscopic dimensions easily inhalable. Exposure to asbestos fibers, both for occupational and non-occupational reasons, has been linked to numerous health problems and respiratory diseases. The earliest reports of asbestos-related disease were from France and the United Kingdom in 1906 (Murray, 1990). In 1927, the terms “asbestosis” and “asbestos bodies” were used for the first time in English (Cooke, 1927) and in 1950, the relation between exposure to asbestos and lung cancer and mesothelioma became known (Wagner et al., 1960). Today, three principal diseases are linked to asbestos exposure: (1) *Asbestosis*, a non-malignant diffuse interstitial fibrosis of the lung tissue; (2) *Lung cancers* related to asbestos exposure: bronchogenic carcinomas, which include squamous cell carcinomas, small- and large-cell carcinoma, and adenocarcinomas; (3) *Mesothelioma*, a cancer which develops mainly in the pleura (outer lining of the lungs and internal chest wall), but it may also occur in the pericardium and peritoneum (the lining of heart and abdominal cavities, respectively). The main features of such tumors are: long latency, difficult diagnosis, and capability of appearing even after the inhalation of an extremely low asbestos concentration, known as a triggering dose (U.S. National Research Council, 1985). Epidemiological studies show that low to moderate exposure to chrysotile asbestos presents a very low health risk, and this is presumably due to its solubility in the body. On the contrary, the bio-solubility of amphibole asbestos is very low (Van Oss et al., 1999; Wood et al., 2006).

The mechanism through which asbestos fibers may give rise to disease is not yet completely clear. Toxicological studies show that interactions between fibrous material and biological environment are strongly dependent on both the geometry and the crystal chemistry of mineral fibers (Stanton et al., 1981; Bonneau et al., 1986a; Fubini, 1993, 1996; Gilmour et al., 1997). In particular, the presence and the bioavailability of iron have received considerable attention by the biomedical community. It was proposed that both the presence and structural coordination of iron are important factors in the toxicity of asbestos (Bonneau et al., 1986b) and, furthermore, that only the Fe

* Corresponding author. Fax: +39 06 4454 729.
E-mail address: alessandro.pacella@uniroma1.it (A. Pacella).

0009-2541/$ – see front matter © 2010 Elsevier B.V. All rights reserved.
doi:10.1016/j.chemgeo.2010.07.018

exposed on the fiber surface or released into the liquid medium by leaching phenomenon is relevant in the Reactive Oxygen Species (ROS) production (Zalma et al., 1987a; Pezerat et al., 1989; Fubini and Mollo, 1995; Favero-Longo et al., 2005; Gazzano et al., 2005). The formation of ROS is of crucial relevance, because it determines a strong release of HO° free radicals by partially dissolving into biological fluids, as described by the Fenton reaction (Kane et al., 1996; Fubini and Otero Arean, 1999; Kamp and Weitzman, 1999; Robledo and Mossman, 1999).

Investigations on the relations between asbestos exposure and related diseases have focused mainly on working exposures. However, as previously mentioned, asbestos also occurs as accessory minerals in several rocks. In ophiolite complexes, the most abundant of these rocks, chrysotile, tremolite and actinolite asbestos frequently occur (Ross and Nolan, 2003). The term "ophiolite" indicates fragments of oceanic lithosphere obducted onto the edges of continental plates. Ophiolitic rocks are commonly used as building and ornamental materials because of their physical and mechanical qualities such as strength, durability, and variety in appearance and color. Epidemiological studies showed an unusually large occurrence of mesothelioma cases in small villages in Turkey, Greece, Cyprus, Corsica and New Caledonia. All these villages lie within or near to ophiolite complexes, and the residents have been exposed to tremolite and actinolite asbestos quarried from local rock formations and used as an ingredient for stucco and whitewash (Ross and Nolan, 2003). In addition, fibrous tremolite and actinolite asbestos also occur in the ophiolite complexes of the USA, particularly in Virginia, Maryland, Pennsylvania and in California (El Dorado County). In such localities, due to the possible health effects that the mineral dust may have on the local residents, an asbestos exposure control plan has been instituted (Ross and Nolan, 2003).

In the Italian peninsula, especially in the Alps and the Apennines, there are abundant ophiolitic outcrops rich in serpentine (some of which may occur as chrysotile) and amphibole (some of which may occur as fibers of tremolite–actinolite and anthophyllite). The Piedmont region (NW Italy) has the largest number of such outcrops, as for example the Lanzo Valley (particularly Balangero mine, where chrysotile was mined) and the Susa Valley. High environmental concern was recently caused by the excavations of railway tunnels in the Susa Valley. In fact, some high-speed railway lines such as Turin–Lyon and Genoa–Milan involve tunnel excavations occurring in metamorphic rocks (serpentinites) containing fibrous tremolite. These excavations gave rise to worker health and public environmental issues for their potential harmful effects on human health (Piolatto et al., 1990; Astolfi et al., 1991; Ballirano et al., 2008). Fibers of tremolite from Ala di Stura (Lanzo Valley, Piedmont) were used in an intraperitoneal injection experiment with male SPF Wistar rats: the tremolite showed high carcinogenicity and very long incubation time of the mesothelioma (Davis et al., 1991; Addison and McConnel, 2005). In addition to the Alps and Apennines, ophiolites hosting fibers of tremolite also outcrop at many localities in the central and southern part of Italy. Quarries of ophiolite, widely used in the past, are present in the regions of Latium (Burragato et al., 2001) and Calabria (Punturo et al., 2004) but their presence has not been associated with health problems so far. Conversely, in the Basilicata region, the presence of fibrous tremolite in the soils of the towns Lauria and Castelluccio Superiore (Potenza) has been related to some pleural mesothelioma cases occurred in these rural communities (Pasetto et al., 2004).

Tremolite is a monoclinic (C2/m) calcic amphibole with ideal formula $^{A}\square^{B}Ca_2^{C}Mg_5^{T}Si_8O_{22}^{O3}(OH)_2$. The C2/m amphibole structure consists of two principal components: a double chain of corner-sharing tetrahedra and a strip of edge-sharing octahedra, both of which extending in the *c*-direction and forming the "I-beam" blocks (Fig. 1a, b). Both tetrahedrally-coordinated sites are denoted as T, and the octahedrally coordinated sites are denoted as M. There are two distinct tetrahedra designated as T(1) and T(2) and three distinct types of octahedra designated as M(1), M(2) and M(3). The double chain of tetrahedra and the strip of octahedra are linked by the M(4) site. The A site occurs below the hexagonal ring of tetrahedra, at the center of a large cavity. The crystal chemistry of prismatic varieties of the various amphiboles has been described in thousands of papers (see reviews by Hawthorne, 1981, 1983; Hawthorne and Oberti, 2007) whereas that of the asbestiform varieties, in spite of the large concerns associated with them, has been addressed only in a few cases (for example: Sokolova et al., 2000, 2001; Gunter et al., 2003; Gianfagna et al., 2003, 2007; Ballirano et al., 2008; Pacella et al., 2008; Bandli et al., 2003; Sanchez and Gunter, 2008; Sanchez et al., 2008).

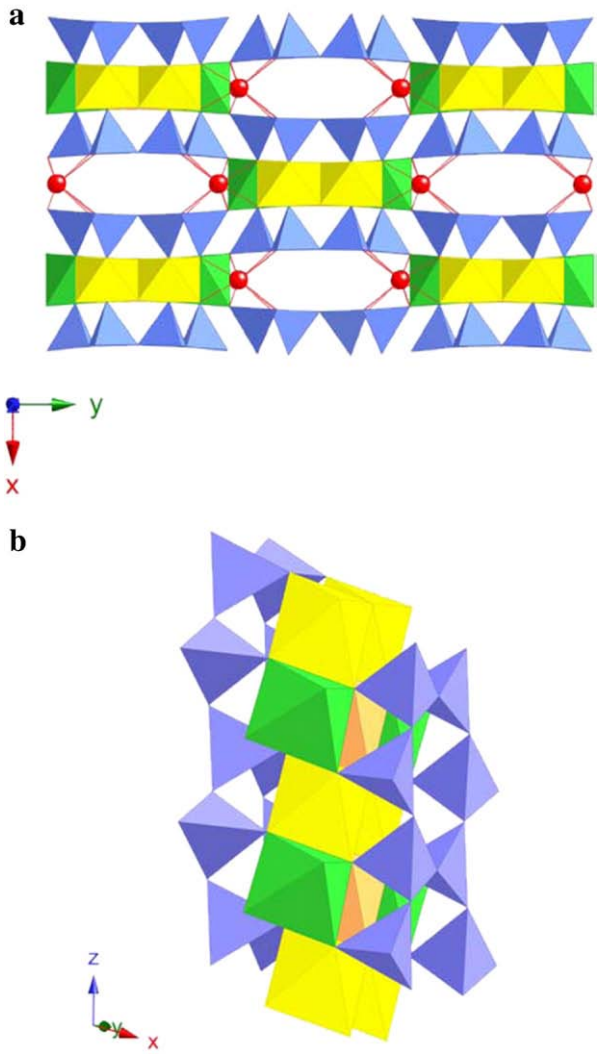

Fig. 1. C2/m amphibole structure. a): projection onto (001) showing the "I-beam" blocks linked by M(4) sites; b): "I-beam" block showing the double chain of tetrahedra and the strip of octahedra elongated in the *c*-direction. Yellow = M(1), green = M(2), orange = M(3), and red = M(4).

The present study is devoted to the full characterization of tremolite asbestos occurring in its natural setting by means of a well tested multi-analytical approach, with the intent of unraveling correlations between crystal chemistry and chemical reactivity.

2. Materials and analytical methods

2.1. Materials

Three specimens come from different ophiolitic outcrops of central and southern part of Italy: 1) Mt. Rufeno, Acquapendente, Latium;

2) Castelluccio Superiore, Potenza, Basilicata; and 3) San Mango, Catanzaro, Calabria. In addition, another sample coming from the ophiolite complex outcropping in Maryland (Montgomery County, Maryland, USA) was studied. Data for a fibrous tremolite from Ala di Stura (Lanzo Valley, Piedmont, Italy) were used for comparison, as this sample was previously studied by Pacella et al. (2008).

2.2. Analytical methods

2.2.1. Scanning electron microscopy (SEM), electron microprobe analysis (EMPA) and inductively coupled plasma-mass spectrometry (ICP-MS)

Scanning electron microscopy was done using a ZEISS DSM 940A equipped with a LINK energy-dispersive system (EDS) for microanalysis and a Philips XL30 equipped with EDAX EDS. Images were obtained from a fragment of the hand specimen mounted on a sample stub and carbon coated. Analytical conditions were: 15 kV accelerating voltage and 3.4 μA beam current. The chemical composition of tremolite fibers was determined using a Cameca SX-50 electron microprobe equipped with five wavelength-dispersive spectrometers at the following conditions: excitation voltage 15 kV accelerating voltage, specimen current 15 nA, beam diameter 5 μm, 20 s counting time (peak), and 10 s counting time (background). The following standards were used: wollastonite (Si Kα, Ca Kα), rutile (Ti Kα), corundum (Al Kα), magnetite (Fe Kα), metallic Mn (Mn Kα), periclase (Mg Kα), orthoclase (K Kα), jadeite (Na Kα), metallic Cr (Cr Kα) fluorophlogopite (F Kα) and sylvite (Cl Kα). The crystal chemical formulae were normalized on the basis of 24 (O + F + Cl). Cations are reported in atoms per formula unit (apfu) and were assigned, following Hawthorne (1981), to the four A, B, C and T groups, filled according to the order recommended by Leake et al. (1997).

2.2.2. ^{57}Fe Mössbauer spectroscopy (MS)

The amphibole fibers were ground gently in an agate mortar with acetone and mixed with a powdered acrylic resin to avoid (or reduce) preferred orientation. About 100 mg of sample were available, so that the absorber was within the limits for the thin-absorber thickness described by Long et al. (1983). Data were collected at room temperature using a conventional spectrometer system operated in constant acceleration mode with a ^{57}Co source of nominal strength of 50 mCi in rhodium matrix, and recorded in a multichannel analyzer using 512 channels for the velocity range −4 to 4 mm/s. After velocity calibration against a spectrum of high-purity α-iron foil (25 μm thick), the raw data were folded to 256 channels. The spectrum was fitted using the Recoil 1.04 fitting program (Lagarec and Rancourt, 1998). A first cycle of refinement was done by fitting pure Lorentzian line-shapes, but the Lorentzian line-shapes showed wide half-widths. Therefore, a second cycle of refinement was done by fitting quadrupole-splitting distributions (QSD), following the approach of Gunter et al. (2003) and Gianfagna et al. (2007). A number of fitting models with unconstrained parameters [isomer shift (δ_0), coupling parameter (δ_1), center of Gaussian component (Δ_0), Gaussian width (σ_Δ), and absorption area (A)] were tried in order to obtain the best fit. A model based on two sites ($1Fe^{2+} + 1Fe^{3+}$), each with two components, was finally chosen. The increasing of the number of Gaussian components did not change the resulting distribution significantly. The uncertainties calculated using the covariance matrix were estimated as no less than ±3% for both Fe^{2+} and Fe^{3+} absorption areas.

2.2.3. Fourier-transform infrared (FT-IR) spectroscopy

FT-IR data were collected on a Nicolet MAGNA 760 over the range of 4000–400 cm^{-1}: 32 scans at a nominal resolution of 4 cm^{-1} were averaged. The instrument was equipped with a KBr beamsplitter and a TGS detector. The powdered samples were mixed in a 2:100 ratio with 200 mg of KBr in order to obtain transparent pellets. Measurements were done in air at room temperature.

2.2.4. X-ray Powder Diffraction (XRPD)

Powder diffraction data were collected on a fully automated parallel-beam Bruker AXS D8Advance diffractometer, operating in transmission mode, and equipped with a Position Sensitive Detector (PSD) VÅNTEC-1. Fibers were ground under ethanol in an agate mortar and the powder was mounted in a 0.7 mm diameter borosilicate–glass capillary. Rietveld refinement was done with the GSAS suite of programs (Larson and Von Dreele, 1985) using the EXPGUI graphical user interface (Toby, 2001). The background was fitted with a Chebyshev polynomial (from 25 to 36-terms) of the first kind to model the amorphous contribution arising from the capillary. Peak-shape was fitted with the TCH pseudo-Voight function (Thompson et al., 1987) modified for asymmetry (Finger et al., 1994). Refined variables were GW (angle-independent) Gaussian parameter, LX, LY (1/cosθ and tanθ dependent) Lorenzian parameters, and S/L and H/L asymmetry parameters (constrained to be equal in magnitude). Starting structural data for the fibers were those of Yang and Evans (1996). Isotropic-displacement parameters were kept fixed at the reference values throughout the refinement. Cell parameters, fractional coordinates for all the atoms, and site scattering for M(1), M(2), M(3), M(4) and M(4′) were refined for the fibers. The geometry of the system was partly restrained under the following conditions: T–O × 8 = 1.625(25) Å, O–O × 12 = 2.655(40) Å, M(1)–O × 6 = 2.08(1) Å, M(2)–O × 6 = 2.08(5) Å, M(3)–O × 6 = 2.07(1) Å, M(4)–O × 8 = 2.51(15) Å, M(4′)–O × 8 = 2.55(35) Å with an initial weight on the constraints of 1000. The weight associated with those observations was progressively reduced to 2 at the last stages of the refinement. The presence of preferred orientation was modeled using the generalized spherical-harmonic descriptions of Von Dreele (1997).

2.2.5. Determination of HO° radicals by electron paramagnetic resonance (EPR) spectroscopy

Reactivity tests on the Italian samples (Mt. Rufeno, Castelluccio Superiore, San Mango, and Ala di Stura) were done in a reactor kept at constant temperature of 37 °C by water flow. The reactor was placed on a swinging table in order to ensure the continuous agitation of the reagents. The reaction takes place in an aerobic medium and protected from the light. All solutions were prepared in a phosphate buffer (pH = 7.4, 0.5 mol/l) obtained from disodium hydrogen phosphate (Na_2HPO_4, Sigma, 99% in purity) and sodium dihydrogen phosphate (NaH_2PO_4, Sigma, 99% in purity). The solid sample (25 mg) was introduced into the reactor together with 0.5 ml of sodium phosphate buffer solution at pH = 7.4 (0.5 mol/l), 1 ml of aqueous buffered solution of 5.5-dimethyl-1-pyrroline-N-oxide (DMPO) as a spin-trapping agent (10^{-1} mol/l) and 0.5 ml of buffered H_2O_2 (0.6%/vol) obtained after dilution of commercial solution (Prolabo "Normapur", 30% in volume). The DMPO solution was obtained from commercial DMPO (Aldrich, 97% in purity) previously purified on activated carbon (Prolabo). All studied samples were ground in an agate mortar for 1 min just before the assay. It must be noted that the grinding operation is not perfectly reproducible, as it depends on the operator, on the morphology of the particle, and on the amount of the starting solid. Part of the suspension was drawn after 5 and 30 min and filtered on a cellulose acetate filter of 0.22 μm. Finally, the solution was injected in a flat quartz cuvette and used for EPR analysis. Duplicate tests were performed for all samples in order to obtain statistically significant results. Reference tests on solutions without samples were also performed in order to check the quality of the reactants.

EPR spectra of radical adduct (DMPO, HO)° were obtained at room temperature using a Brucker ESP-300E spectrometer and are in agreement with those given in the literature (Zalma et al., 1987b).

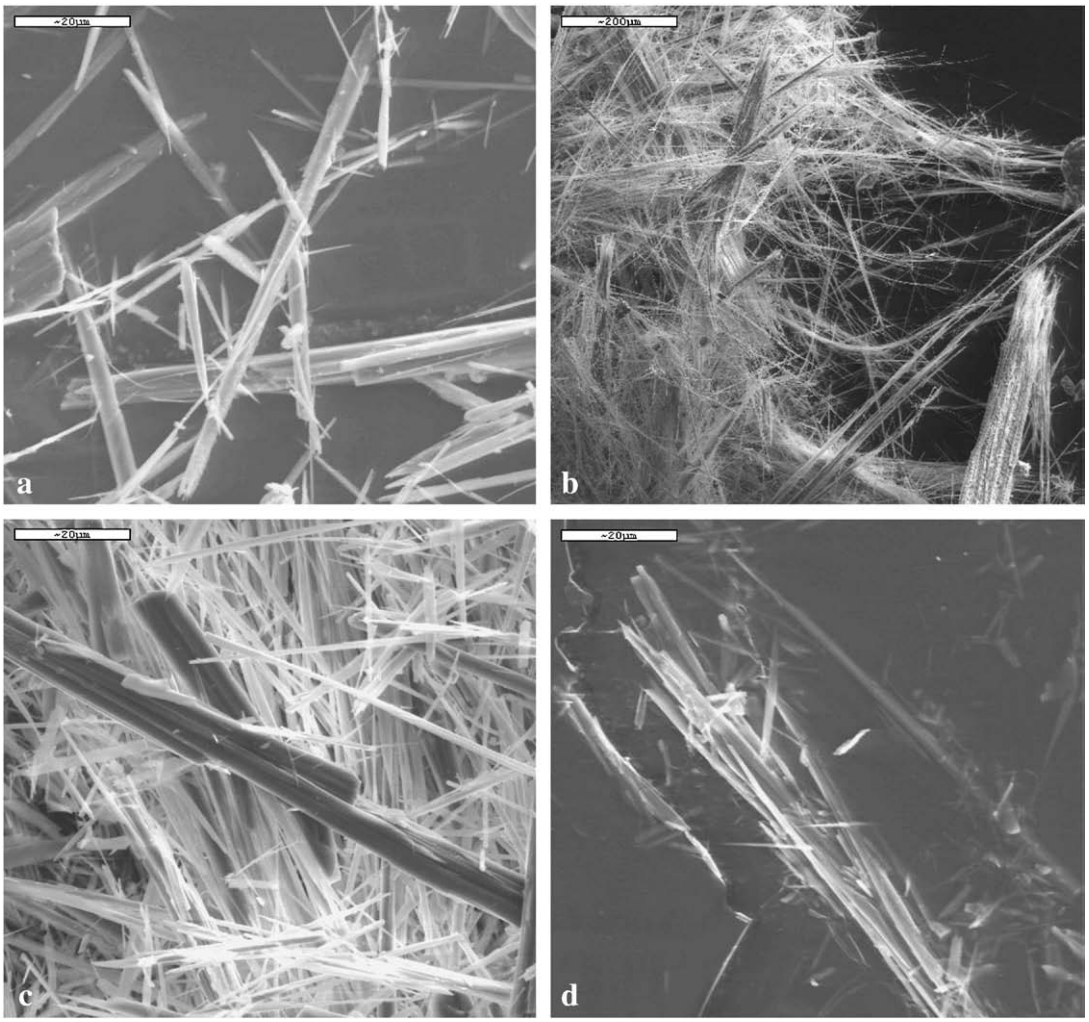

Fig. 2. SEM images of fibrous tremolite samples: a) Mt. Rufeno, b) Castelluccio Superiore, c) San Mango, and d) Maryland. Dimension bar: 200 μm.

Analytical conditions were: magnetic field 3440 G, frequency field 9.65 GHz, power 10 mW, frequency modulation 100 KHz, constant time 1 s, modulation amplitude 3.24 G and gain of 5 10^4, acquisition time 84.92 ms. Each spectrum is composed of 4 lines with a coupling constant (a_N and a_H) of 14.9 G (Janzen and Ping Liu, 1973). To obtain the corrected intensity (I, expressed in arbitrary unit, a.u.), the

Table 1
Average chemical compositions obtained by EMP and ICP-MS analysis for the investigated fibrous tremolite samples (estimated standard deviations in brackets). Reference data of a fibrous tremolite from Ala di Stura (Pacella et al., 2008) are shown for comparison.

	Mt. Rufeno		Castelluccio		San Mango		Maryland		Ala di Stura	
Oxides (wt.%)	EMP	ICP	EMP	ICP	EMP	ICP	EMP	ICP	EMP	ICP
SiO_2	56.75(42)	–	58.04(47)	–	58.53(64)	–	57.42(36)	–	57.50(36)	–
TiO_2	0.03(2)	0.02	0.02(2)	0.03	0.01(1)	0.01	0.03(2)	0.04	0.02(2)	0.02
Al_2O_3	0.55(7)	0.02	0.16(4)	0.30	0.07(7)	0.50	0.09(4)	0.15	0.05(1)	0.04
Cr_2O_3	0.03(2)	–	0.01(2)	–	0.01(2)	–	–	–	0.01(1)	–
MgO	22.13(28)	24.00	23.36(22)	24.09	22.81(31)	21.71	21.71(58)	21.28	22.64(22)	28.01
CaO	12.23(13)	9.41	12.67(24)	12.84	13.43(28)	15.46	13.45(19)	14.06	13.14(13)	15.79
MnO	0.10(4)	0.12	0.13(4)	0.10	0.08(3)	0.09	0.13(5)	0.11	0.26(5)	0.19
FeO_{tot}	2.23(8)	2.90	2.06(16)	2.02	2.97(9)	2.94	4.50(77)	4.18	2.42(25)	2.27
Na_2O	0.37(4)	0.11	0.23(3)	0.22	0.06(2)	0.11	0.02(1)	0.04	0.06(2)	0.03
K_2O	0.02(1)	0.03	0.06(2)	0.05	0.02(1)	0.01	0.01(1)	0.04	0.03(1)	0.02
F	0.05(5)	–	0.04(6)	–	0.04(5)	–	0.03(5)	–	0.04(5)	–
Cl	0.02(1)	–	0.01(1)	–	0.01(1)	–	0.00(1)	–	0.01(1)	–
H_2O[a]	2.10		2.14		2.16		2.14		2.13	
	96.61		98.94		100.2		99.54		98.3	
F,Cl = O	0.02		0.02		0.02		0.01		0.02	
Total	96.59		98.92		100.18		99.53		98.28	
Fe_2O_3[b]	0.60		0.48		0.20		0.80		0.32	
FeO[b]	1.70		1.63		2.80		3.78		2.13	

[a] Estimated from stoichiometry.
[b] Measured by Mössbauer spectroscopy.

Table 2
Average crystal chemical formulas of the investigated fibrous tremolite samples. Reference data of a fibrous tremolite from Ala di Stura (Pacella et al., 2008) are shown for comparison.

Sites	Mt. Rufeno	Castelluccio	San Mango	Maryland	Ala di Stura
Si	7.988	7.989	8.000	7.953	7.992
^{IV}Al	0.012	0.011	0.000	0.015	0.008
$\sum$T	8.000	8.000	8.000	7.968	8.000
^{VI}Al	0.079	0.015	0.011	0.000	0.000
Ti	0.003	0.002	0.001	0.003	0.002
Cr	0.003	0.001	0.001	0.000	0.001
Fe^{3+}	0.064	0.050	0.021	0.083	0.033
Mg	4.643	4.793	4.648	4.482	4.691
Fe^{2+}	0.200	0.188	0.320	0.438	0.248
Mn	0.012	0.015	0.009	0.015	0.031
$\sum C$	5.005	5.064	5.011	5.022	5.005
ΔC	0.005	0.064	0.011	0.022	0.005
Ca	1.845	1.869	1.967	1.996	1.957
Na	0.101	0.061	0.016	0.005	0.015
K	0.004	0.011	0.003	0.002	0.005
$\sum B$	1.954	2.005	1.997	2.025	1.983
OH	1.974	1.967	1.971	1.974	1.977
F	0.022	0.017	0.017	0.013	0.018
Cl	0.005	0.002	0.002	0.000	0.002
$\sum O_3$	2.001	1.986	1.991	1.987	1.996
Ca/$\sum$M[a]	0.37	0.37	0.39	0.40	0.39
X_{FeA}(%)[b]	4.4	4.1	6.6	9.2	5.6

[a] $M = Mg + Fe^{2+} + Mn + Ni + Ti + {}^{VI}Fe^{3+} + {}^{VI}Cr^{3+} + {}^{VI}Al$.
[b] Ferro-actinolite content: $X_{FeA} = (Fe^{2+} + Mn)/(Fe^{2+} + Mn + Mg)$.

average value calculated on the spectra collected after 5 and 30 min (from the beginning of the reaction) was reduced by the value obtained for the control.

3. Results

The samples studied here show variable morphology. Acicular morphology and fiber bundles are evident from electron micrographs at different magnifications (Fig. 2), with the fibers showing a thickness even lower than 1 μm (200 to 600 nm). In particular, Mt. Rufeno, San Mango and Maryland samples are characterized by an acicular–fibrous morphology, whereas Castelluccio Superiore sample shows a more filamentous–asbestiform morphology.

The EMP analyses revealed substantial chemical homogeneity with the exception of Fe content. In particular, the Italian tremolite samples have variable Fe content, in the order of San Mango > Ala di Stura > Rufeno > Castelluccio Superiore, but the sample from Maryland shows a Fe content almost double that of the Italian samples (Table 1). Notably, results obtained on Maryland tremolite are in very good agreement with previous chemical analysis by Sanchez and Gunter (2008). For San Mango and Mt. Rufeno samples, comparison between bulk (ICP-MS) and point (EMP) chemical results reveals MgO and CaO differences which are far larger than the standard deviations. However, these differences are not due to chemical inhomogeneities, but are related to the presence of serpentine and calcite in the hand sample, as further confirmed by XRPD. All samples show a Ca/ΣM ratio very close to that of the ideal tremolite (Ca/ΣM = 0.40) and have crystal chemical formula close to the nominal formula of tremolite, $\square Ca_2Mg_5Si_8O_{22}(OH)_2$ (Table 2). Due to their variable Fe content (0.2–0.5 apfu), they belong to the tremolite–actinolite–ferro-actinolite series.

The Mössbauer spectrum of a fibrous tremolite is typical of a paramagnetic material (Fig. 3), and is composed of two main contributions (Table 3). The first contribution is centered at δ_0 of 1.1 mm/s and is due to Fe^{2+}: it was reproduced by two well-defined components, with quadrupole-splitting distributions centered at Δ_0 1.9 and 2.9 mm/s, respectively (Fig. 4a). The second contribution is centered at δ_0 0.30 mm/s and is due to Fe^{3+}: being very different from sample to sample, it was tentatively modeled with two components, a narrow component at 1 mm/s and a broad component (Fig. 4b). The Fe^{3+}/Fe_{tot} ratio was quantified on the basis of spectral absorption areas (Fe^{3+}_{raw}). To account for the temperature effect, the empirical factor of Dyar et al. (1993) was applied, and the corrected Fe^{3+} ratio (Fe^{3+}_{corr}) was obtained. The values obtained range from 6% Fe_{tot} (San Mango tremolite) to 24% Fe_{tot} (Mt. Rufeno tremolite).

According to the refined Δ_0 values and areas of different Fe^{2+} components, in all samples about 40% of the total Fe^{2+} was assigned to the M(2) site, and the remaining 60% at the M(1) + M(3) sites. In the tremolite–actinolite series, Burns and Greaves (1971) attributed the Fe^{2+} doublets with quadrupole splitting of 1.7–1.9 mm/s and 2.8–2.9 mm/s to Fe^{2+} at M(2) and Fe^{2+} at M(1) sites, respectively. More recently, many authors have agreed to assign the doublets with the lowest quadrupole-splitting values to Fe^{2+} at M(2), but different assignments were proposed for the doublets with the highest quadrupole-splitting values, often suggesting an irresolvable combination of Fe^{2+} at M(1) + M(3) sites (Ballirano et al., 2008; Gunter et al., 2003). The presence of Fe^{2+} at M(1) and M(3) is also confirmed by the FT-IR spectra (Fig. 5). In fact, in addition to the typical absorption band at 3673–3675 cm^{-1} assigned to the arrangement $^{M(1)}Mg^{M(1)}Mg^{M(3)}Mg$, a well developed band is observed at 3660 cm^{-1}, and only for San Mango and Maryland tremolites, a very weak band is

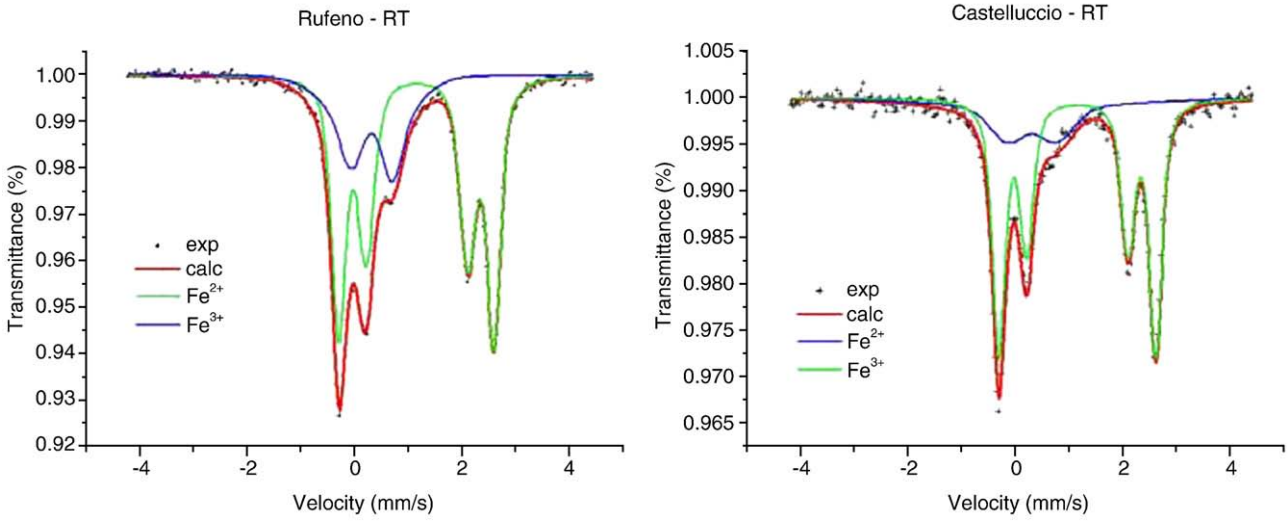

Fig. 3. Room-temperature ^{57}Fe Mössbauer spectrum of two fibrous tremolite samples with different ferrous:ferric ratios (fitting by QSD).

Table 3
^{57}Fe Mössbauer hyperfine parameters at room temperature for the investigated fibrous tremolite samples. Fitting approach: quadrupole-splitting distributions (QSD). Symbols according to Rancourt and Ping (1991).

Sample	χ^2	Fe^{2+}				Fe^{3+}				Fe^{3+}_{raw}	Fe^{3+}_{corr}
		δ_0 (mm/s)	Δ_0 (mm/s)	σ_Δ (mm/s)	Area (%)	δ_0 (mm/s)	Δ_0 (mm/s)	σ_Δ (mm/s)	Area (%)	(% Fe_{tot})	(% Fe_{tot})
Mt. Rufeno	0.65	1.18	1.89	0.21	32	0.35	0.76	0.31	14	28	24
		1.18	2.89	0.16	40	0.35	1.07	0.86	14		
Castelluccio	0.94	1.14	1.89	0.16	30	0.30[a]	0.90	0.57	14	24	21
		1.14	2.92	0.13	46	0.30[a]	1.69	3.21	10		
San Mango[b]	0.83	1.19	1.89	0.17	34	0.30[a]	1.32	0.97	6	7	6
		1.19	2.91	0.15	59	0.30[a]	6.06	0.00	1		
Ala di Stura[b]	0.79	1.19	1.89	0.20	37	0.25	1.02	0.32	8	15	12
		1.19	2.92	0.17	48	0.25	2.16	0.62	7		
Maryland[b]	1.46	1.19	1.90	0.18	33	0.30[a]	1.30	1.46	15	18	16
		1.19	2.90	0.17	49	0.30[a]	6.06	0.61	3		

Notes: Isomer shift (δ_0) with respect to α-iron; δ_1 always lower than 0.05; $\gamma = 0.194$ mm/s; $h_+/h_- = 1$. The Fe^{3+}_{raw} is obtained from the area of absorption peaks assigned to Fe^{3+}. The Fe^{3+}_{corr} is obtained from the raw value by applying the correction factor $C = 1.22$ (Dyar et al., 1993). Estimated uncertainties are about 0.02 mm/s for hyperfine parameters, and no less than 3% for absorption areas (expressed as % of Fe_{tot}).
[a] Kept fixed throughout the refinement.
[b] Original data in Fantauzzi et al. (2010).

also observed at 3645 cm^{-1}. Both additional bands were attributed to the presence of Fe^{2+} at M(1) and M(3) according to the results of Skogby and Rossman (1991) and Hawthorne and Della Ventura (2007). Moreover, the absence in the FT-IR spectrum of absorption bands at $\Delta = -50$ cm^{-1} from the tremolite reference band allowed to assignment of Fe^{3+} to only M(2), as previously suggested by Raudsepp et al. (1987). This is consistent with our Mössbauer results, for which both Fe^{3+} components were assigned to the M(2) site, following results previously

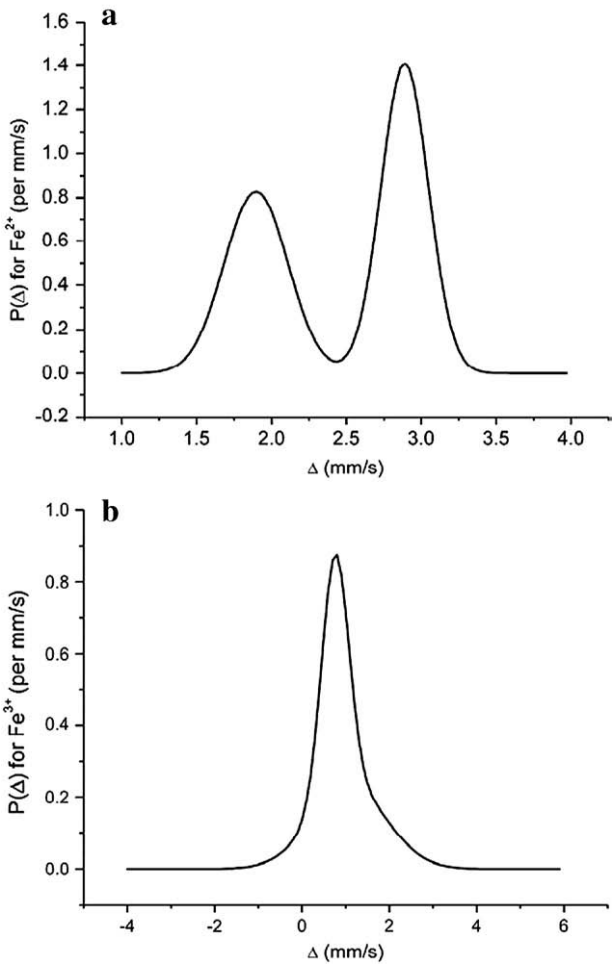

Fig. 4. Probability–density distributions [P(Δ)] for: a) Fe^{2+} and b) Fe^{3+} as obtained from QSD fitting. Example from Mt. Rufeno tremolite.

reported by various authors for sodic amphiboles (Ernst and Wai, 1970), strontian potassicrichterite (Sokolova et al., 2000), ferrian winchite (Sokolova et al., 2001), winchite–richterite (Gunter et al., 2003), fluoro–edenite (Gianfagna et al., 2007) and tremolite (Ballirano et al., 2008). In particular, the very large component observed in our Mössbauer spectra (Fig. 4b) could be caused by crystal size or isolated magnetic states for Fe^{3+}, as suggested by Gunter et al. (2003), or alternatively by other cations locally disordered around Fe^{3+}, as already observed in fibrous amphiboles (Andreozzi et al., 2009) and other complex silicates (Andreozzi et al., 2004, 2008).

Preliminary evaluation of the diffraction pattern indicated the presence of serpentine (a reflection at 12.5° was removed from the refinement) in the Ala di Stura (Pacella et al., 2008) and Mt. Rufeno samples, in addition to 10 wt.% calcite (included in the refinement) in the San Mango sample. Convergence was reached with the agreement factors reported in Table 4, where the data for Castelluccio Superiore sample are shown as an example. Results showed that, except for Mt. Rufeno tremolite, the cell volume measured for the other fibrous samples (Table 5) is always higher than the values reported in literature: for prismatic tremolite: 906–907 $Å^3$ (Gottschalk et al., 1999; Verkouteren and Wylie, 2000; Yang and Evans, 1996); for fibrous tremolite: 907.37 $Å^3$ (Ballirano et al., 2008). The high volumes here observed are due to the presence of ferro-actinolite content, ranging in our samples from 4 to 9%. In addition, the lower volume observed for Mt. Rufeno tremolite is in agreement with its highest content of smaller high-charge cations (Al^{3+} and Fe^{3+}) at the C-group (Table 2). Selected bond distances and fractional coordinates are available from the authors on request. The <T(1)–O> distances observed for all samples are similar, and are always slightly smaller than <T(2)–O>, as commonly reported for C2/m amphiboles with no tetrahedrally-coordinated Al (Hawthorne, 1981). Polyhedral distortion Δ shows comparable values for both T(1)- and T(2) tetrahedra. No correlations between for the <M(1)–O>, <M(2)–O> and <M(3)–O> distances have been attempted because their differences are scattered widely within two standard deviations of an individual bond distance. Refined site scattering (s.s.) obtained for M(1), M(2) and M(3) sites for all studied samples indicates the presence of a scatterer cation heavier than Mg. The agreement between s.s. refined and those calculated from chemical data is quite satisfactory, the largest difference being ca. 4% relative for Castelluccio and Maryland tremolites (Table 6).

The EPR measurements (Fig. 6) for all samples showed evidence of chemical reactivity in the formation of the hydroxyl radical, in the presence of H_2O_2, with differences larger than their standard deviations (Fig. 6). In particular, the lowest value obtained for the Castelluccio Superiore sample, and the highest for the San Mango sample. The sample from Maryland (value not given) was measured

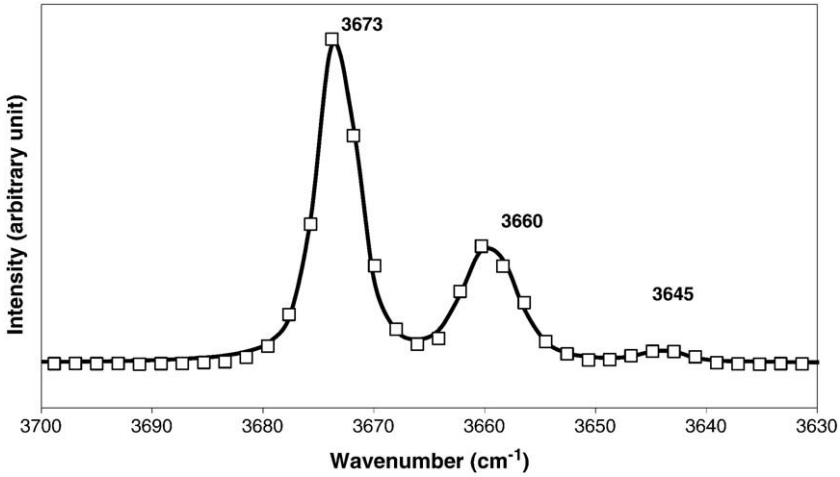

Fig. 5. FT-IR spectrum in the 3700–3600 cm^{-1} range of the investigated fibrous tremolite. Example from San Mango tremolite.

with a different EPR apparatus (and thus with different analytical conditions) together with the sample from San Mango (re-measured as reference sample). The two samples showed comparable chemical activity in the production of the HO° radical.

4. Discussion

Assigned site populations of the investigated samples were derived by combining chemical and structural data (Table 6). By Mössbauer analysis, Fe^{2+} was preliminarily attributed to M(2) and to an irresolvable combination of [M(1) + M(3)] sites. As a second step, on the basis of the total amount of Fe^{2+} obtained from the chemical formula and according to the refined site-scattering values, the fractions of Fe^{2+} at M(1) and at M(3) are ca. 67% and ca. 33%, respectively. As the M(1) and M(2) multiplicities are twice that of M(3), for all samples Fe^{2+} turns to be disordered over the M(1), M(2) and M(3) sites. However, the M(2) site is much more Fe-enriched than M(1) and M(3), the former showing Fe-site occupancies from 7% to 13% (due to both Fe^{2+} and Fe^{3+}), and the latter showing Fe-site occupancies from 4% to 9% (due to only Fe^{2+}). Notably, this is in full agreement with results obtained for tremolite–ferro-actinolite series by Evans and Yang (1998) and for fibrous tremolite by Ballirano et al. (2008).

Table 4
Experimental details of the X-ray diffraction data collection and miscellaneous data of the refinement for the investigated fibrous tremolite samples. Statistical descriptor as defined by Young (1993). Example from Castelluccio sample.

Castelluccio	
Instrument	Siemens D8 Advance
X-ray tube	CuKα at 40 kV and 40 mA
Incident beam optic	Multilayer X-ray mirrors
Sample mount	Rotating capillary (60 rpm)
Soller slits	2 (2.3° divergence + radial)
Divergence and antidivergence slits	0.6 mm
Detector	Position sensitive detector (PSD) VÅNTEC-1 opening window 6° 2θ.
2θ range (°)	5–140
Step size (°)	0.02
Counting time (s)	10
R_p (%); R_{wp} (%); R_F (%)	1.51; 2.21; 2.55
Reduced χ2	6.06
Restraints contribution to χ2	84.5
Refined parameters	87
Peak-cut-off (%)	0.05
J	1.001
GW	22.1(5)
LX, LY	6.2(1), 6.6(1)
S/L = H/L	0.0233(2)

Table 5
Unit-cell parameters of fibrous tremolite samples. Reference data of a fibrous tremolite from Ala di Stura (Pacella et al., 2008) and of a prismatic tremolite, Y&E96 (Yang and Evans, 1996) are shown for comparison.

	a (Å)	*b* (Å)	*c* (Å)	β (°)	*V* (Å^3)
Mt. Rufeno	9.8354(3)	18.0567(6)	5.2775(2)	104.664(3)	906.72(6)
Castelluccio	9.8477(1)	18.0623(2)	5.28086(4)	104.742(1)	908.40(2)
San Mango	9.8474(1)	18.0753(2)	5.28246(4)	104.758(1)	909.23(1)
Maryland	9.8538(2)	18.0709(2)	5.27903(6)	104.738(1)	909.09(2)
Ala di Stura	9.8424(1)	18.0712(2)	5.28354(7)	104.680(1)	909.07(2)
Y&E96	9.8356(12)	18.0557(22)	5.2785(6)	104.782(9)	906.4(2)

Table 6
Site-scattering (s.s.) values in electrons per formula unit for the investigated fibrous tremolite samples, obtained from the structure refinement (left) and calculated from the assigned site population (right).

	s.s. from refinement	Assigned site population	s.s. from assigned site population
Mt. Rufeno			
M(4)	39.24(28)	$Ca_{1.84}$; $Na_{0.10}$; $Mn_{0.01}$	38.15
B site sum	**39.24(28)**		**38.15**
M(1)	24.38(26)	$Mg_{1.92}$; $Fe^{2+}_{0.08}$	25.12
M(2)	25.75(24)	$Mg_{1.76}$; $Fe^{3+}_{0.06}$; $Fe^{2+}_{0.08}$; $Al_{0.08}$	25.80
M(3)	13.46(18)	$Mg_{0.96}$; $Fe^{2+}_{0.04}$	12.56
C site sum	**63.59(40)**		**63.48**
Castelluccio			
M(4)	39.03(12)	$Ca_{1.87}$; $Na_{0.06}$; $K_{0.01}$; $Mn_{0.01}$; $Mg_{0.05}$	39.15
B site sum	**39.03(12)**		**39.15**
M(1)	24.18(10)	$Mg_{1.92}$; $Fe^{2+}_{0.08}$	25.12
M(2)	24.17(10)	$Mg_{1.87}$; $Fe^{3+}_{0.05}$; $Fe^{2+}_{0.07}$; $Al_{0.01}$	25.69
M(3)	12.43(7)	$Mg_{0.96}$; $Fe^{2+}_{0.04}$	12.56
C site sum	**60.78(16)**		**63.37**
San Mango			
M(4)	38.92(12)	$Ca_{1.97}$; $Na_{0.02}$; $Mn_{0.01}$	39.87
B site sum	**38.92(12)**		**39.87**
M(1)	25.01(12)	$Mg_{1.87}$; $Fe^{2+}_{0.13}$	25.82
M(2)	24.48(12)	$Mg_{1.84}$; $Fe^{3+}_{0.02}$; $Fe^{2+}_{0.13}$ $Al_{0.01}$	26.11
M(3)	12.70(8)	$Mg_{0.94}$; $Fe^{2+}_{0.06}$	12.84
C site sum	**62.19(19)**		**64.31**
Maryland			
M(4)	39.36(16)	$Ca_{1.99}Na_{0.01}$; $Mn_{0.02}$	40.39
B site sum	**39.36(16)**		**40.39**
M(1)	25.97(14)	$Mg_{1.82}$; $Fe^{2+}_{0.18}$	26.52
M(2)	25.49(14)	$Mg_{1.75}$; $Fe^{3+}_{0.08}$; $Fe^{2+}_{0.17}$	27.50
M(3)	13.27(11)	$Mg_{0.91}$; $Fe^{2+}_{0.09}$	13.26
C site sum	**64.73(23)**		**67.28**

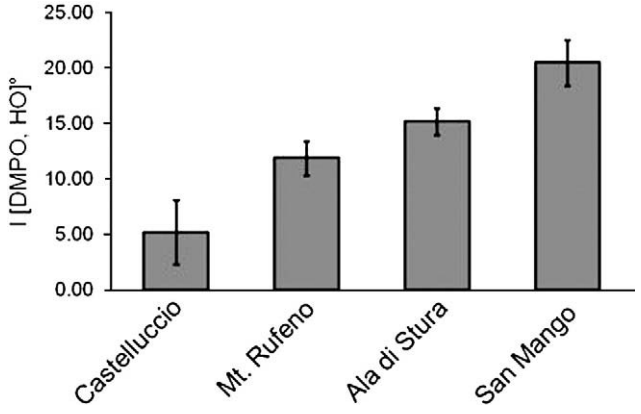

Fig. 6. Intensity of the signal (DMPO, HO)°, measured for the Italian fibrous tremolite samples in presence of H_2O_2 in buffered phosphate medium (pH 7.4). The intensity is reported in arbitrary unit. Error bars correspond to $\pm 1\sigma$.

It has been accepted that not only the Fe content, but also its position in the structure play a relevant role in the interaction between fibers and biological environment, being only the Fe exposed at the surface responsible for the chemical reactivity (Shukla et al., 2003; Gazzano et al., 2005; Favero-Longo et al., 2005). The mineral surfaces are usually related to mineral cleavage, but in the case of fibers, the sites exposed on the surfaces are strictly dependent on the fiber morphology (Brown and Gunter, 2003). In fact, Wylie (1979) and Verkouteren and Wylie (2002) reported that amphibole fibers are composed of smaller, parallel fibrils tightly packed and randomly oriented around a common elongation, the *c* axis. Considering that the amphibole structure is made of "I-beam" blocks extending in the *c*-direction and linked by M(4) sites (Fig. 1a), each fibril is therefore composed of a number of "I-beams" (Fig. 1b), exhibiting M(1) and M(2) octahedra on external surfaces. Moreover, as mentioned above, the multiplicity of the M(1) and M(2) sites is twice that of M(3), and hence the Fe at M(1) and M(2) has a higher probability of being involved in surface reactions than Fe at M(3).

4.1. Asbestos reactivity: is iron content a proxy?

In mineral fibers, there is toxicological evidence that iron may trigger carcinogenesis by participating in Fenton chemistry, that is, producing ROS that determines the strong release of HO° free radicals (Zalma et al., 1987a; Kane et al., 1996; Fubini and Otero Arean, 1999; Kamp and Weitzman, 1999; Robledo and Mossman, 1999). As mentioned before, the presence of iron and its coordination environment in the structure are key-factors of fiber bioactivity. The Italian tremolite samples here studied contain low Fe_{tot} (ca. 2–3 wt.%), but are very active in the HO° radical production. For the Italian samples, the quantity of HO° radical produced is directly related to the Fe_{tot} content of the fibers, and linearly correlated with $^{[M(1)+M(2)]}Fe$ content (Fig. 7). Notably, this is in agreement with the Fenton chemistry and further supports the hypothesis that the Fe at M(1) and M(2) sites is active in surface reactions. Moreover, preliminary results of cytotoxicity tests with 3-(4.5-Dimethylthiazol-2-yl)-2.5-diphenyltetrazolium bromide (MTT assay) revealed a significant mortality of the cells kept in contact with these tremolite samples (Gianfagna et al., 2008). In particular, for the San Mango tremolite a particularly high Fe^{3+}/Fe_{tot} ratio occurs at the fiber surface, and this finding was claimed to be responsible for the observed delay of cell mortality (Fantauzzi et al., 2010). It must be noted that in this study, among the different ROS, only the HO° radicals were determined. Moreover, it is known that other very electrophilic oxygen species, not radical and as reactive as the HO° radicals [e.g., iron oxo entities such as Fe(IV) = O, Fe(VI) = O, and many more], are also able to affect the cytotoxicity (Nejjari et al., 1993).

In conclusion, the combined approach adopted here consisting in the full characterization of fibrous amphiboles coupled with reactivity studies and toxicity tests, has shown itself very powerful, since it was able to shed new light on the role of Fe in the interaction between fibers and organic environment.

Acknowledgments

A. Gianfagna is thanked for PhD thesis supervision and financial support of A.P., L. Stievano for useful suggestions and advices, P. Ballirano for XRPD data collection, and G. Della Ventura for FT-IR data collection. M. Serracino is thanked for technical assistance during EMP analysis at CNR–Instituto di Geologia Ambientale e Geoingegneria, and C. Cremisini for ICP-MS analyses at ENEA–Centro Ricerche Casaccia. F. Burragato and L. Papacchini kindly provided the Castelluccio Superiore and Mt. Rufeno samples, J. Addison the Ala di Stura sample, and M.E. Gunter the Maryland sample. The authors are very grateful to M.E. Gunter and F.C. Hawthorne for their useful and constructive suggestions, and to J. Snelleman for the careful handling of the manuscript.

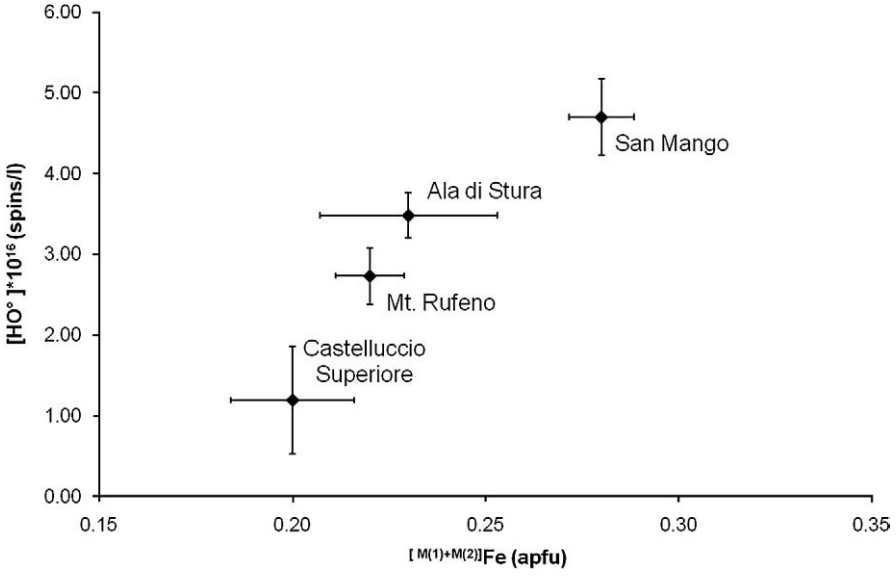

Fig. 7. [HO°] formation from the Italian fibrous tremolite samples in relation to their $^{[M(1)+M(2)]}Fe$ content.

Finally, A.P. and G.B.A. are grateful to F. Bosi for his pleasant company during the manuscript development.

References

Addison, J., McConnel, E.E., 2005. A review of carcinogenicity studies of asbestos and non-asbestos tremolite and other amphiboles. International Symposium on the Health Hazard Evaluation of Fibrous Particles associated with Taconite and the adjacent Duluth Complex.

Andreozzi, G.B., Lucchesi, S., Graziani, G., Russo, U., 2004. Site distribution of Fe^{2+} and Fe^{3+} in axinite mineral group: the new crystal-chemical formula. Am. Mineral. 89, 1763–1771.

Andreozzi, G.B., Bosi, F., Longo, M., 2008. Linking Mössbauer and structural parameters in elbaite–schorl–dravite tourmalines. Am. Mineral. 93, 658–666.

Andreozzi, G.B., Ballirano, P., Gianfagna, A., Mazziotti-Tagliani, S., Pacella, A., 2009. Structural and spectroscopic characterization of a suite of fibrous amphiboles with high environmental and health relevance from Biancavilla (Sicily, Italy). Am. Mineral. 94, 1333–1340.

Astolfi, A., Belluso, E., Ferraris, G., Fubini, B., Giamello, E., Volante, M., 1991. Asbestiform minerals associated with chrysotile from Western Alps (Piedmont–Italy): chemical characteristics and possible related toxicity. In: Brown, R.C., Hoskins, J.A., Johnson, N.F. (Eds.), Mechanisms in Fiber Carcinogenesis, Life Sciences. : NATO ASI Series A, 223. Plenum Press, New York, pp. 269–283.

Ballirano, P., Andreozzi, G.B., Belardi, G., 2008. Crystal chemical and structural characterization of fibrous tremolite from Susa Valley, Italy, with comments on potential harmful effects on human health. Am. Mineral. 93, 1349–1355.

Bandli, B.R., Gunter, M.E., Twamley, B., Foit Jr., F.F., Cornelius, S.B., 2003. Optical, compositional, morphological, and X-ray data on eleven particles of amphibole from Libby, Montana, U.S.A. Can. Mineral. 41, 1241–1253.

Bonneau, L., Malard, C., Pezerat, H., 1986a. Studies on surface properties of asbestos. 2. Role of dimensional characteristics and surface properties of mineral fibers in the induction of pleural tumors. Environ. Res. 41, 268–275.

Bonneau, L., Suquet, H., Malard, C., Pezerat, H., 1986b. Studies on surface properties of asbestos. 1. Active sites on surface of chrysotile and amphiboles. Environ. Res. 41, 251–267.

Brown, B.M., Gunter, M.E., 2003. Morphological and optical characterization of amphiboles from Libby, Montana U.S.A. by Spindle Stage Assisted - Polarized Light Microscopy. Microscope 15, 121–140.

Burns, R.G., Greaves, C., 1971. Correlations of infrared and Mössbauer site population measurements of actinolites. Am. Mineral. 56, 2010–2033.

Burragato, F., Ballirano, P., Fiori, S., Papacchini, L., Sonno, M., 2001. Segnalazione di tremolite asbestiforme nel Lazio. Il Cercapietre Notiziario del Gruppo Mineralogico Romano 1–2, 33–35.

Cooke, W.E., 1927. Pulmonary asbestosis. Br. Med. J. 2, 1024–1025.

Davis, J.M.G., Addison, J., McIntosh, C., Miller, B.G., Niven, K., 1991. Variations in the carcinogeneticy of tremolite dust samples of differing morphology. Ann. NY Acad. Sci. 643, 473–490.

Dyar, M.D., Mackwell, S.M., McGuire, A.V., Cross, L.R., Robertson, J.D., 1993. Crystal chemistry of Fe^{3+} and H^{+} in mantle kaersutite: implications for mantle metasomatism. Am. Mineral. 78, 968–979.

Ernst, W.G., Wai, C.N., 1970. Mössbauer, infrared, X-ray and optical study of cation ordering and dehydrogenation in natural and heat-treated sodic amphiboles. Am. Mineral. 55, 1226–1258.

Evans, B.W., Yang, H., 1998. Fe-Mg order–disorder in tremolite–actinolite–ferro-actinolite at ambient and high temperature. Am. Mineral. 83, 458–475.

Fantauzzi, M., Pacella, A., Atzei, D., Gianfagna, A., Andreozzi, G.B., Rossi, A., 2010. Combined use of X-ray photoelectron and Mössbauer spectroscopic techniques in the analytical characterization of iron oxidation state in amphibole asbestos. Anal. Bioanal. Chem. 396, 2889–2898.

Favero-Longo, S.E., Castelli, D., Salvadori, O., Belluso, E., Piervittori, R., 2005. Pedogenetic action of the lichens *Lecidea atrobrunnea*. *Rhizocarpon geographicum* gr. and *Sporastatia testudinea* on serpentinized ultramafic rocks in an alpine environment. Int. Biodeterior. Biodegrad. 56, 17–27.

Finger, L.W., Cox, D.E., Jephcoat, A.P., 1994. A correction for powder diffraction peak asymmetry due to axial divergence. J. Appl. Crystallogr. 27, 892–900.

Fubini, B., 1993. The possible role of surface chemistry in the toxicity of inhaled fibers. In: Wahreit, D.B. (Ed.), Fiber Toxicology, 11. Academic Press, San Diego, pp. 229–257.

Fubini, B., Mollo, L., 1995. Role of iron in the reactivity of mineral fibers. Toxicol. Lett. 82–83, 951–960.

Fubini, B., 1996. Physico-chemical and cell free assays to evaluate the potential carcinogenicity of fibres. In: Kane, A.B., Boffetta, P., Saracci, R., Wilbourn, J. (Eds.), Mechanisms of Fibre Carcinogenesis. IARC Scientific Publication, Lyon, p. 140.

Fubini, B., Otero Arean, C., 1999. Chemical aspects of the toxicity of inhaled mineral dusts. Chem. Soc. Rev. 28, 373–381.

Gazzano, E., Riganti, C., Tomatis, M., Turci, F., Bosia, A., Fubini, B., Ghigo, D., 2005. Potential toxicity of nonregulated asbestiform minerals: balangeroite from the western Alps. Part 3: depletion of antioxidant defenses. J. Toxicol. Environ. Health 68, 41–49.

Gianfagna, A., Ballirano, P., Bellatreccia, F., Bruni, B.M., Paoletti, L., Oberti, R., 2003. Characterization of amphibole fibers linked to mesothelioma in the area of Biancavilla, Eastern Sicily, Italy. Mineral. Mag. 67, 1221–1229.

Gianfagna, A., Andreozzi, G.B., Ballirano, P., Mazziotti-Tagliani, S., Bruni, B.M., 2007. Structural and chemical contrasts between prismatic and fibrous fluoro-edenite from Biancavilla, Sicily, Italy. Can. Mineral. 45, 249–262.

Gianfagna, A., Andreozzi, G.B., Ballirano, P., Pacella, A., Mazziotti-Tagliani, S., Bruni, B.M., Paoletti, L., Cardile, V., Pugnaloni, A., Giantomassi, F., Fournier, J., Stievano, L., 2008. Characterization of fibrous tremolites of environmental and health interest. 33rd International Geological Congress. Session Earth and Health–Medical Geology, Oslo, Norway. # MGH-01835P (abstr.).

Gilmour, P.S., Brown, D.M., Beswik, P.H., Macnee, W., Rahman, I., Donaldson, K., 1997. Free radical activity of industrial fibers: role of iron in oxidative stress and activation of transcription factors. Environ. Health Perspect. 105 (Suppl. 5), 1313–1317.

Gottschalk, M., Andrut, M., Melzer, S., 1999. The determination of the cummingtonite content of synthetic tremolite. Eur. J. Mineral. 11, 967–982.

Gunter, M.E., Dyar, M.D., Twamley, B., Foit Jr., F.F., Cornelius, C., 2003. Composition, $Fe^{3+}/\Sigma Fe$, and crystal structure of non-asbestiform and asbestiform amphiboles from Libby, Montana, U.S.A. Am. Mineral. 88, 1970–1978.

Hawthorne, F.C., 1981. Crystal chemistry of the amphiboles. In: Veblen, D.R. (Ed.), Amphiboles and Other Hydrous Pyriboles Mineralogy Reviews in Mineralogy, 9A. Mineralogical Society of America, 1–102.

Hawthorne, F.C., 1983. The crystal chemistry of the amphiboles. Can. Mineral. 21, 173–480.

Hawthorne, F.C., Della Ventura, G., 2007. Short range order in amphiboles. In: Hawthorne, et al. (Eds.) Amphiboles: Crystal chemistry, Occurrence, and Health Issues, Rev. Mineral. Geochem, vol. 67. Mineralogical Society of America, pp. 173–222.

Hawthorne, F.C., Oberti, R., 2007. Amphiboles: Crystal Chemistry. In: Hawthorne, et al. (Eds.) Amphiboles: Crystal chemistry, Occurrence, and Health Issues, Rev. Mineral. Geochem, vol. 67. Mineralogical Society of America, pp. 1–54.

Janzen, E.G., Ping Liu, J.I., 1973. Radical addition reactions of 5.5-dimethyl-1-pyrroline-1-oxide, ESR spin trapping with a cyclic nitrone. J. Magn. Reson. 9, 510–512.

Kamp, D.W., Weitzman, S.A., 1999. The molecular basis of asbestos induced lung injury. Thorax 54, 638–652.

Kane, A.B., Boffetta, P., Wilbourn, J.D., 1996. Mechanisms of Fibre Carcinogenesis: IARC Scientific Publication, 140.

Lagarec, K., Rancourt, D.G., 1998. RECOIL. Mössbauer Spectral Analysis Software for Windows, Version 1.0. Department of Physics, University of Ottawa, Canada.

Larson, A.C., Von Dreele, R.B., 1985. General structure analysis system (GSAS). Los Alamos National Laboratory Report LAUR 86-748.

Leake, B.E., Woolley, A.R., Arps, C.E.S., Birch, W.D., Gilbert, M.C., Grice, J.D., Hawthorne, F.C., Kato, A., Kisch, H.J., Krivovichev, V.G., Linthout, K., Laird, J., Mandarino, J.A., Maresch, V.W., Nickel, E.H., Rock, N.M.S., Schumacher, J.C., Smith, D.C., Stephenson, N.N., Ungaretti, L., Withtaker, E.J.W., Youzhi, G., 1997. Nomenclature of amphiboles: report of the subcommittee on amphiboles of the International Mineralogical Association, Commission on New Minerals and Mineral Names. Am. Mineral. 82, 1019–1037.

Long, G.J., Cranshaw, T.E., Longworth, G., 1983. The ideal Mössbauer effect absorber thickness. Mössbauer Eff. Ref. Data J. 6, 42–49.

Murray, R., 1990. Asbestos: a chronology of its origins and health effects. Br. J. Ind. Med. 47, 361–365.

Nejjari, A., Fournier, J., Pezerat, H., Leanderson, P., 1993. Mineral fibres: correlation between oxidising surface activity and DNA base hydroxylation. Occup. Environ. Med. 50, 501–504.

Pacella, A., Andreozzi, G.B., Ballirano, P., Gianfagna, A., 2008. Crystal chemical and structural characterization of fibrous tremolite from Ala di Stura (Lanzo Valley, Italy). Per. Mineral. 77, 51–62.

Pasetto, R., Bruni, B.M., Bruno, C., D'Antona, C., De Nardo, P., Di Maria, G., Di Stefano, R., Fiorentini, C., Gianfagna, A., Marconi, A., Paoletti, L., Putzu, M.G., Soffritti, M., Comba, P., 2004. Problematiche sanitarie della fibra anfibolica di Biancavilla. Aspetti epidemiologici, clinici e sperimentali. Note dell' Istituto Superiore di Sanità 17, 8–12.

Pezerat, H., Zalma, R., Guignard, J., Jaurand, M.-C., 1989. Production of oxygen radicals by the reduction of oxygen arising from the surface activity of mineral fibres. In: Bignon, J., Peto, J., Saracci, R. (Eds.), Non Occupational Exposure to Mineral Fibers, 90. IARC Scientific Publication, Lyon, pp. 100–110.

Piolatto, G., Negri, E., La Vecchia, C., Pira, E., Decarli, A., Peto, J., 1990. An update of cancer mortality among chrysotile asbestos miners in Balangero, Northern Italy. Br. J. Ind. Med. 47, 810–814.

Punturo, R., Fiannacca, P., Lo, Giudice A., Pezzino, A., Cirrincione, R., Liberi, F., Piluso, E., 2004. Le Cave storiche della "Pietra Verde" di Gimigliano e Monte Reventino (Calabria): studio petrografico e geochimico. Bollettino della Società Gioenia di Scienze Naturali 37, 37–59.

Rancourt, D.G., Ping, J.Y., 1991. Voigt-based methods for arbitrary-shape static hyperfine parameter distributions in Mössbauer spectroscopy. Nucl. Instrum. Methods Phys. Res. B58, 85–97.

Raudsepp, M., Turnock, A.C., Hawthorne, F.C., Sherriff, B.K., Hartman, J.S., 1987. Characterization of synthetic pargasitic amphiboles ($NaCa_2Mg_4M^{3+}Si_6Al_2O_{22}(OH, F)_2$; M^{3+}=Al, Cr, Ga, Sc, In) by infrared spectroscopy, Rietveld structure refinement, and ^{27}Al, ^{29}Si, and ^{19}F MAS NMR spectroscopy. Am. Mineral. 72, 580–593.

Robledo, R., Mossman, R., 1999. Cellular and molecular mechanisms of asbestos-induced fibrosis. J. Cell. Physiol. 180, 158–166.

Ross, M., Nolan, R.P., 2003. History of asbestos discovery and use and asbestos-related disease in context with the occurrence of asbestos within ophiolite complexes. Geol. Soc. Am. Spec. Pap. 373.

Sanchez, M.S., Gunter, M.E., 2008. Tests of the correlation between composition and morphology of tremolite from Montgomery County, Maryland, USA. Per. Mineral. 77, 13–23.

Sanchez, M.S., Gunter, M.E., Dyar, M.D., 2008. Characterization of historical amphibole samples from the former vermiculite mine near Libby, Montana, USA. Eur. J. Mineral. 20, 1043–1053.

Shukla, A., Gulumian, M., Hei, T.K., Kamp, D., Rahman, Q., Mossman, B.T., 2003. Serial review: Role of reactive oxygen and nitrogen species (ROS/RNS) in lung injury and diseases. Multiple roles of oxidants in the pathogenesis of asbestos-induced diseases. Free Radical Biol. Med. 34, 1117–1129.

Stanton, M.F., Layard, M., Tegeris, A., Miller, E., May, M., Morgan, E., Smith, A., 1981. Relation of particle dimension to carcinogenicity in amphibole asbestoses and other fibrous minerals. J. Natl Cancer Inst. 67, 965–975.

Sokolova, E.V., Kabalov, Y.K., McCammon, C., Schneider, J., Konev, A.A., 2000. Cation partitioning in an unusual strontian potassicrichterite from Siberia: Rietveld structure refinement and Mössbauer spectroscopy. Mineral. Mag. 64, 19–23.

Sokolova, E.V., Hawthorne, F.C., McCammon, C., Schneider, J., 2001. Ferrian winchite from the Ilmen Mountains, Southern Urals, Russia and some problems with the current scheme of nomenclature. Can. Mineral. 39, 171–177.

Skogby, H., Rossman, G.R., 1991. The intensity of amphibole OH bands in the infrared absorption spectrum. Phys. Chem. Miner. 18, 64–68.

Thompson, P., Cox, D.E., Hastings, J.B., 1987. Rietveld refinement of Debye–Scherrer synchrotron X-ray data from Al_2O_3. J. Appl. Crystallogr. 20, 79–83.

Toby, B.H., 2001. EXPGUI, a graphical user interface for GSAS. J. Appl. Crystallogr. 34, 210–213.

U.S. National Research Council, 1985. Asbestiform Fibres: Non-Occupational Health Risks. National Academy Press, Washington. 352 p.

Van Oss, C.J., Naim, J.O., Costanzo, P.M., Giese Jr., R.F., Wu, W., Sorling, A.F., 1999. Impact of different asbestos species and other mineral particles on pulmonary pathogenesis: clay. Clay Min. 47, 697–707.

Verkouteren, J.R., Wylie, A.G., 2000. The tremolite–actinolite–ferro-actinolite series: systematic relationship among cell parameters, composition, optical properties, and habit, and evidence of discontinuities. Am. Mineral. 85, 1239–1254.

Verkouteren, J.R., Wylie, A.G., 2002. Anomalous optical properties of fibrous tremolite, actinolite, and ferro-actinolite. Am. Mineral. 87, 1090–1095.

Von Dreele, R.B., 1997. Quantitative texture analysis by Rietveld refinement. J. Appl. Crystallogr. 30, 517–525.

Wagner, J.C., Sleggs, C.A., Marchand, P., 1960. Diffuse pleural mesothelioma and asbestos exposure in the Northwestern Cape Province:. Br. J. Ind. Med. 17, 260–271.

Wylie, A.G., 1979. Optical properties of the fibrous amphiboles. Annals of the New York Academy of Sciences 330, 600–605.

Wood, S.A., Taunton, A.E., Normand, C., Gunter, M.E., 2006. Mineral–fluid interaction in the lungs: insights from reaction-path modeling. Inhal. Toxicol. 18, 975–984.

Yang, H., Evans, B.W., 1996. X-ray structure refinements of tremolite at 140 and 295 K: crystal chemistry and petrologic implications. Am. Mineral. 81, 1117–1125.

Young, R.A., 1993. Introduction to the Rietveld method. In: Young, R.A. (Ed.), The Rietveld Method. Oxford Science, Oxford, pp. 1–38.

Zalma, R., Bonneau, L., Guignard, J., Pezerat, H., Jaurand, M.-C., 1987a. Production of hydroxyl radicals by iron solid compounds. Toxicol. Environ. Chem. 13, 171–187.

Zalma, R., Bonneau, L., Guignard, J., Pezerat, H., Jaurand, M.-C., 1987b. Formation of oxy radicals by oxygen reduction arising from the surface activity of asbestos. Can. J. Chem. 67, 2338–2341.